Soliton interactions on dual-core fibers

S. L. Doty
Department of Science and Math, GMI Management and Engineering Institute, Flint, Michigan 48504-4898

J. W. Haus, YunJe Oh, and R. L. Fork
Department of Physics, Rensselaer Polytechnic Institute, Troy, New York 12180
(Received 23 June 1994; revised manuscript received 26 September 1994)

Dynamics of ultrashort pulse propagation in a dual-core fiber are governed by a set of coupled nonlinear Schrödinger equations. We apply numerical and analytical techniques to study the nature of the inelastic interactions between identical soliton pulses propagating in close proximity on separate cores. We find that the soliton interactions can change from repulsive at small values of the coupling coefficient to attractive at large values. Representative experimental parameters are discussed.

PACS number(s): 42.81.Qb, 42.50.Rh, 42.65.−k

INTRODUCTION

Future communication systems are expected to operate at terabit data rates. These high data rates, combined with a need for high reliability and precise timing, suggest that soliton interactions, and, in particular, transmission and switching of solitons propagating in parallel, are an important topic of investigation. Just as individual solitons offer an integrity of the basic unit of information, the interactions of pairs of solitons may offer unique opportunities for realizing stable relationships of solitons.

We devote our attention in this article to interactions that are expected to arise between solitons on adjacent cores of a dual-core fiber in order to evaluate their prospects for use in all optical switching or gating devices. This work differs from previous work on pulse switching in nonlinear directional couplers [1–3] in that we consider using the interaction as a means of rearranging the temporal position of a pulse in its bit window as opposed to launching a pulse on one core and switching that pulse to the adjacent core.

In 1989, Abdullaev, Abrarov, and Darmanyan (AAD) [4] examined theoretically the interaction forces between pulses launched on adjacent cores of a dual-core fiber. These interactions were shown to be similar in nature and behavior to interactions observed between solitons propagating on the same single-mode, single-core fiber [5,6]. AAD addressed this problem analytically by invoking an inverse scattering perturbation technique. The results displayed both attractive and repulsive interactions between solitons on adjacent cores of a dual-core fiber.

A frequency shift in the power spectrum of a soliton can alter its velocity. It is helpful to keep in mind that the physical influence between two solitons occurs due to the evanescent-field coupling. The interaction force is a result of the asymmetry in the self-phase modulation at the leading and trailing edges of the pulse caused by the influence of the evanescent field of one pulse overlapping with the other pulse. The spectral shifts change the pulse velocity because of the medium dispersion. Since the solitons are robust and readjust their shape under the action of the perturbation, the complex physical changes due to the field coupling are closely modeled by an effective force concept.

In this paper we present work that extends the investigation of dual-core soliton interactions begun by AAD. Our approach is both analytical and numerical. We invoke a variational formalism involving trial functions in order to describe the main characteristics of the pulse evolution as determined by the coupled nonlinear Schrödinger equations (CNLSEs). A complimentary analysis of the Hamiltonian system is presented which correlates well with the results found from the variational analysis. Our results are confirmed and expanded by the use of numerical simulations which indicate the extent to which the variational method may be used to model such problems. We find results similar to, but not in exact agreement with, those of AAD. Moreover we explore effects which, to our knowledge, have not been previously reported and are absent from AAD's treatment.

The work is organized as follows. In Sec. I the CNLSEs are introduced, the variational formulation is developed, an investigation of the global dynamics of the system is explored through a Hamiltonian analysis, and the analytical results are presented. In Sec. II details regarding the numerical analysis and the computational algorithm for solving the CNLSEs are outlined. In Sec. III we discuss the main results via a comparison between the predictions made from the variational analysis, the published results of AAD, and the results of numerical simulations.

I. ANALYTICAL METHODS

In the past, variational approaches have provided accurate information regarding the propagation of pulses

under the action of the NLSEs [7–9]. This method can likewise be applied to the CNLSEs [3,10]. The "action" integral is constructed with a Lagrangian function. The Euler-Lagrange equations that extremize the action correspond to the CNLSEs. By appropriately choosing the field's trial functions, which contain several variational parameters, the action is optimized using a Rayleigh-Ritz procedure. This yields the closest solution of the problem consistent with the trial function. Although successful implementation critically depends on the trial function, this method has the advantage of providing analytical expressions for the pulse evolution.

Once chosen, the trial function cannot change its shape. The parameters form a system of ordinary differential equations, which, in general, necessitate recourse to numerical tools. Although the new system of ordinary differential equations may be less demanding computationally than the original system of partial differential equations, we cannot obtain analytical solutions unless further simplifications are made. Such simplifications are typically chosen to examine more closely a physical situation of interest.

A. Variational analysis

To begin the variational analysis, we first identify the set of equations (CNLSEs). In our problem we assume that effects on any optical pulse in the first core due to the of the existence of the second core can be represented by introducing a linear coupling to the field on the second core [4,11]:

$$\frac{\partial \psi_1}{\partial \xi} = \frac{i}{2}\frac{\partial \psi_1}{\partial \tau^2} + i\left|\psi_1\right|^2 \psi_1 + i\epsilon\psi_2, \tag{1}$$

$$\frac{\partial \psi_2}{\partial \xi} = \frac{i}{2}\frac{\partial \psi_2}{\partial \tau^2} + i\left|\psi_2\right|^2 \psi_2 + i\epsilon\psi_1, \tag{2}$$

where ϵ is the linear coupling coefficient and the physical parameters are scaled to soliton units [12,13]. In these units, time is scaled to a pulse width T_0 and the electric field envelopes are scaled by an amplitude E_0, i.e., $E_j = E_0\psi_j$, where $j = 1, 2$ labels the core. The amplitude and pulse width of a fundamental soliton are related by

$$|\beta_2| = n_2 k_0 E_0^2 T_0^2, \tag{3}$$

where β_2 is the group velocity dispersion, n_2 is the nonlinear Kerr coefficient, and k_0 is the free-space wave number.

The coupling coefficient in units of inverse meters is approximately expressed as [11]

$$\epsilon = \sqrt{\frac{\pi\Delta n}{n_{\text{core}} l \rho_0 W}}\,\frac{U^2}{V^3 K_1^2(W)}\exp\left(-\frac{Wl}{\rho_0}\right). \tag{4}$$

In Eq. (4), Δn is the refractive index difference between the fiber core(s) and the cladding, n_{core} is the core's refractive index, ρ_0 is the core radius, and l is the center to center separation between the fibers. The modified Bessel function appears in the denominator; $K_1(W)$ and the remaining parameters V, U, and W are related such that

$$\begin{aligned} V &= \frac{2\pi\rho_0}{\lambda}\sqrt{2n_{\text{core}}\Delta n}, \\ U &= \sqrt{1 + 2\ln V}, \\ W &= \sqrt{V^2 - U^2}. \end{aligned} \tag{5}$$

Values for the coupling coefficient are sensitive to the choice of separation between the fibers, as well as the wavelength. Table I provides typical values of the coupling coefficient as a function of core separation, assuming two different values for the pulse duration T_0. The calculations presume a fundamental soliton launched in silica fiber.

Equations (1) and (2) are formulated as a variational problem such that

$$\delta \int\int \mathcal{L} dz d\tau = 0, \tag{6}$$

with the appropriate choice of Lagrangian density $\mathcal{L}$. We find that the appropriate Lagrangian density is given by

$$\begin{aligned} \mathcal{L} = {} & i(\psi_1\psi_{1z}^* - \psi_{1z}\psi_1^*) + i(\psi_2\psi_{2z}^* - \psi_{2z}\psi_2^*) \\ & + (|\psi_{1\tau}|^2 - |\psi_1|^4) + (|\psi_{2\tau}|^2 - |\psi_2|^4) \\ & + 2\epsilon(\psi_1^*\psi_2 + \psi_2^*\psi_1). \end{aligned} \tag{7}$$

The asterisk denotes complex conjugation and the subscripts z and τ denote partial derivatives. The original system of equations Eqs. (1) and (2) are then derived from Euler-Lagrange equations for each field ψ_i such that

$$\frac{\partial}{\partial z}\left(\frac{\partial \mathcal{L}}{\partial \psi_{iz}^*}\right) + \frac{\partial}{\partial \tau}\left(\frac{\partial \mathcal{L}}{\partial \psi_{i\tau}^*}\right) - \frac{\partial \mathcal{L}}{\partial \psi_i^*} = 0, \tag{8}$$

where $\psi_i = \psi_1$ or ψ_2.

Our interest in this approach is to uncover the dynamics of soliton-soliton interactions between pulses residing on adjacent cores in a dual-core fiber. Here we follow the analysis of Ueda and Kath [3]. In constructing our trial function, we introduce parameters that may be important in this interaction.

TABLE I. Coupling coefficients for soliton pulses of various duration in silica fiber: $\Delta n = 5.00 \times 10^{-3}$, $n_{\text{core}} = 1.44$, $\rho_0 = 4.00$ μm. The beat length is defined as π/ϵ.

l (μm)	ϵ (1 ps)	ϵ (0.25 ps)	Beat length (m)
35.0	17.49	1.09	8.98
3.0	12.75	0.797	12.32
37.0	9.30	0.581	16.90
38.0	6.78	0.424	23.17
39.0	4.95	0.309	31.76
40.0	3.61	0.226	43.51
41.0	2.64	0.165	59.61
42.0	1.92	0.120	81.63
43.0	1.41	0.0879	111.8
44.0	1.03	0.0642	152.9
45.0	0.751	0.0469	209.3

In choosing the envelope function, we note that for the case of interacting solitons on the same core, solutions with hyperbolic secant envelope forms have been found. It seems reasonable to presume, at least initially, that in the case of moderate coupling, a hyperbolic secant form for the envelope is preserved for the pulses on adjacent cores of a dual-core fiber. Finally, for convenience we introduce symmetrical trial functions and variational parameters

$$\psi_1 = \eta \mathrm{sech}\left(\frac{\tau - y}{w}\right) \exp\{i[v(\tau - y) + \sigma]\}, \tag{9}$$

$$\psi_2 = \eta \mathrm{sech}\left(\frac{\tau + y}{w}\right) \exp\{i[-v(\tau + y) + \overline{\sigma}]\}, \tag{10}$$

where η is the amplitude of each wave, $2y$ is the separation of the pulse maxima, $2v$ is the relative velocity of the two fields, and σ and $\overline{\sigma}$ are the phases of the pulses on each core. We further constrain ourselves to the case of $w = 1/\eta$ since we are interested in fundamental solitons launched on the coupled fiber system.

We then proceed to evaluate the integral

$$A = \int \mathcal{L} d\tau. \tag{11}$$

Inserting our trial functions Eqs. (9) and (10) into the Lagrangian $\mathcal{L}$, evaluating Eq. (11), and defining $\Delta\sigma = (\overline{\sigma} - \sigma)$, we obtain

$$A = 4\eta\left[\frac{d\overline{\sigma}}{dz} + \frac{d\sigma}{dz} - 2v\frac{dy}{dz} + v^2 - \frac{1}{3}\eta^2\right] + \frac{8\pi\epsilon\eta\cos(\Delta\sigma)\sin(2vy)}{\sinh(2y\eta)\sinh(\pi v/\eta)}. \tag{12}$$

Upon varying the action with respect to the variables of interest η, w, v, y, σ, and $\overline{\sigma}$, the following equations describing the evolution and motion of the pulses are obtained:

$$\frac{d\eta}{dz} = \frac{2\pi\epsilon\eta\sin(2vy)\sin(\Delta\sigma)}{\sinh(2y\eta)\sinh(\pi v/\eta)}, \tag{13}$$

$$\frac{d\eta}{dz} = -\frac{2\pi\epsilon\eta\sin(2vy)\sin(\Delta\sigma)}{\sinh(2y\eta)\sinh(\pi v/\eta)}, \tag{14}$$

$$\frac{dv}{dz} = -\frac{2\pi\epsilon\cos(\Delta\sigma)}{\sinh(\pi v/\eta)} \times\left[\frac{(v/\eta)\sinh(2y\eta) - \sin(2vy)\cosh(2y\eta)}{\sinh^2(2y\eta)}\right], \tag{15}$$

$$\frac{dy}{dz} = v + \frac{\pi\epsilon\cos(\Delta\sigma)}{\sinh(2y\eta)\sinh^2(\pi v/\eta)}\left[2y\cos(2vy)\sinh(\pi v/\eta) - \frac{\pi}{\eta}\sin(2vy)\cosh(\pi v/\eta)\right]. \tag{16}$$

Note that Eqs. (13) and (14) only differ by a minus sign. The only way that both equations can hold is if both are equal to zero. This can be accomplished by restricting our consideration to those cases where the phase difference is $\Delta\sigma = 0, \pi, 2\pi, ..., m\pi$ and m is an integer. This choice restricts the initial conditions of the phase difference for the two fields. The remaining equations [Eqs. (15) and (16)] define the relative velocity and relative separation of the pulses with respect to a common center.

In the limit of small initial separation, Eqs. (15) and (16) can be used in combination to find an evolution equation which describes the behavior of these pulses as they propagate. Specifically, the equations show how the separation between the pulses evolves during propagation. For small separations and relative velocities, the equations can be linearized and reduced to a second-order differential equation

$$\frac{d^2y}{dz^2} = \alpha y, \tag{17}$$

where

$$\alpha = \frac{4\epsilon\eta^2\cos(\Delta\sigma)}{3}\left(1 - \frac{\pi^2\epsilon\cos(\Delta\sigma)}{3\eta^2}\right). \tag{18}$$

Equation (17) has three distinct regimes. Clearly, when $\Delta\sigma = \pi$ or an odd multiple of π, then $\alpha < 0$ and Eq. (17) is a simple harmonic oscillator equation. The solutions are then sinusoidal or oscillatory in nature. We shall term the conditions which result in this type of solution as the "attractive interaction" since it physically corresponds to the case where pulses oscillate about some common center position as they individually propagate down their own fiber cores. This common center position propagates with the average of the linear group velocities of each of the individual pulses. When $\Delta\sigma = 0$ or an even multiple of π, and $[\epsilon/\eta^2]$ is small, then $\alpha > 0$ and the solutions are exponentially growing. The interaction corresponding to this solution will be termed the "repulsive interaction." The exponentially growing solution physically corresponds to the case where the pulses continuously increase their relative separation as they individually propagate down their own fiber core.

The repulsive regime is fragile and depends on the size of the parameter $[\epsilon/\eta^2]$. When $0 < \epsilon < [3\eta^2/\pi^2]$, the solution is exponential as discussed above. The interaction becomes attractive, however, when $\epsilon > [3\eta^2/\pi^2]$. For the attractive case $\Delta\sigma = 0, m\pi$ (m is an even integer), the period of oscillation is given by $3\pi/\sqrt{\epsilon(\pi^2\epsilon - 3\eta^2)}$. In the case of $\Delta\sigma = \pi, n\pi$ (n is an odd integer), the period of oscillation is given as $3\pi/\sqrt{\epsilon(\pi^2\epsilon + 3\eta^2)}$. A summary of these results are given in Table II.

We can compare these analytical results with those obtained by AAD. As stated earlier, AAD analyzed the same problem using a perturbative technique on the inverse scattering method. The results obtained by AAD are qualitatively similar; however, quantitatively they

TABLE II. Analytical predictions of coupled soliton interactions. ISM is the perturbation on inverse scattering method.

Analytical method	Phase difference ($\Delta\sigma$)	Coupling coefficient	Period or growth time
Repulsive interaction			
Variational analysis	0	$0 < \epsilon < \frac{3\eta^2}{\pi^2}$	$\frac{3}{\sqrt{4\epsilon(3\eta^2-\pi^2\epsilon)}}$
ISM	0	$0 < \epsilon < \infty$	$\sqrt{\frac{3}{4\epsilon\eta^2}}$
Attractive interaction			
Variational analysis	0	$\epsilon > \frac{3\eta^2}{\pi^2}$	$\frac{3\pi}{\sqrt{\epsilon(\pi^2\epsilon-3\eta^2)}}$
Variational analysis	π	$0 < \epsilon < \frac{3\eta^2}{\pi^2}$	$\frac{3\pi}{\sqrt{\epsilon(\pi^2\epsilon+3\eta^2)}}$
ISM	π	$0 < \epsilon < \infty$	$\pi\sqrt{\frac{3}{\epsilon\eta^2}}$

differ from ours. Specifically, AAD's procedure leads to the evolution equation

$$\frac{d^2y}{dz^2} = \frac{4\epsilon\eta^2\cos(\Delta\sigma)}{3}y. \tag{19}$$

This equation for the relative separation of the pulses again yields both an oscillatory and an exponentially decaying solution. However, this is where the similarity ends. AAD's results indicate that for $\Delta\sigma = 0, m\pi$ (m is an even integer), the evolution equation always possesses exponentially growing results. In the case where $\Delta\sigma = \pi, n\pi$ (n is an odd integer), the evolution equation [Eq. (19)] always results in an oscillatory solution with period $\pi\sqrt{3/(\epsilon\eta^2)}$. For ease of comparison, and as a summary, AAD's findings are also summarized in Table II.

The differences are clear. First, AAD predict a period for the attractive interaction which differs from that obtained by the variational analysis. The distinction is most clearly seen in the case of small initial amplitude ($\eta < 1$). Second, AAD predict two distinct classes of behavior (the attractive and repulsive interaction) which depend solely on the initial phase difference of the pulses. In such a case, the only possible manner to change the nature of the interaction is through the introduction of a controlled π phase change on one of the pulses. In contrast, the variational analysis indicates that when pulses are launched on a dual-core fiber with a repulsive interaction (i.e., an exponentially increasing separation of the pulses with respect to a common center), the interaction can become oscillatory if the coupling coefficient is sufficiently large. The value of the coupling coefficient may be altered by a change in the relative separation of the fiber cores, a change in the value of the nonlinear refractive index, or a change in the soliton pulse width T_0. Therefore, the variational analysis indicates that varying either the coupling coefficient or the phase relationship between the pulses could lead to a controllable mechanism for reconfiguring pulse positions.

B. The NLSEs and CNLSEs as a Hamiltonian system

While the variational analysis of the CNLSEs is helpful in deriving a set of ordinary differential equations for the adiabatic variation of a select number of parameters describing soliton propagation in a dual-core fiber, it does not provide a clear physical insight into the global dynamics of the system. To obtain a more general picture, we turn to a Hamiltonian analysis of this problem.

Both the NLSEs and CNLSEs are associated with conservative Hamiltonian systems. Using a suitable choice of soliton parameters, one can obtain evolution equations for the system from the Hamiltonian. This approach is attractive in that an immediate global picture of the pulse dynamics may be obtained by drawing phase-space diagrams. In this section we evaluate the Hamiltonian for our parametrized system and find the phase-space diagrams which describe the pulse dynamics for the dual-core system of interest.

By analogy with classical mechanics, we can define a Hamiltonian density for a system from the known Lagrangian density. This Hamiltonian density will, in turn, be directly related to the energy of the system, which is a conserved quantity and is given as

$$\mathcal{H} = \sum p_i q_{i\tau} - \mathcal{L}. \tag{20}$$

The momenta p_i are given as

$$p_i = \frac{\partial\mathcal{L}}{\partial(q_{i\tau})}, \tag{21}$$

where the q_i correspond to the fields ψ_i and the subscript τ refers to partial differentiation with respect to local time.

In general, the Hamiltonian for the CNLSEs is given by

$$H = H_1 + H_2 + H_{\text{int}}, \tag{22}$$

where

$$H = \int_{-\infty}^{\infty}\mathcal{H}d\tau \tag{23}$$

and

$$H_j = \frac{1}{2}\int_{-\infty}^{\infty}\left(-\left|\frac{\partial\psi_j}{\partial\tau}\right|^2 + |\psi_j|^4\right)d\tau \qquad (j = 1, 2), \tag{24}$$

$$H_{\text{int}} = \int_{-\infty}^{\infty} 2\epsilon\psi_1\psi_2^* \, d\tau. \tag{25}$$

For our ansatz, the choice of $\eta = 1/w$, it can be shown that the CNLSEs obey the first three conservations laws, that is, the total "energy," the "momentum," and the "number of particles" summed over both cores remain a constant. Additionally, for the choice of initial phase difference $\Delta\sigma$ equal to 0 or π, the Hamiltonian is conserved on each individual core.

Utilizing the Lagrangian density found above and Eq. (20), we find the energy for our system to be given by

$$E = 4\eta\left[-v^2 + \frac{\eta^2}{3} - \frac{2\pi\epsilon\cos(\Delta\sigma)\sin(2vy)}{\sinh(2y\eta)\sinh(\pi v/\eta)}\right]. \tag{26}$$

E is constant for a dynamical trajectory in the phase space. We choose the coupling coefficient ϵ, the initial phase difference $\Delta\sigma$, and the initial amplitude η as fixed parameters. This leaves only the relative velocity v and the pulse separation y as free parameters. We can construct a phase-space diagram by plotting the value of the Hamiltonian for various initial conditions of pulse separation y and relative velocity v. We begin by investigating the attractive interaction with coupling coefficients $\epsilon = 0.1$, $\Delta\sigma = \pi$, and $\eta = 1$ in Fig. 1. It should be noted that the trajectories obtained using the Hamiltonian analysis were reconstructed using a direct integration of the coupled equations. The contours are labeled by the value of the energy. Bounded trajectories occur near the origin and unbounded trajectories occur for large relative velocities. For values of the energy above 1.5 we obtain bounded, elliptical orbits. When the value of the energy is 1.4, the phase-space trajectory is distorted indicating a region of transition. For values of the energy below 1.4, the trajectories are unbounded indicating that for sufficiently large initial separation and/or relative velocity the pulses will each retain their own group velocity and maintain their initial separation. This is consistent with our findings in the variational analysis above. [Recall that a condition for obtaining Eq. (17) was the consideration of small initial separation.] As the amplitude of the pulses is increased to 1.5, as shown in Fig. 2, we again find two distinct phase-space trajectories separated by a transition region. However, the conditions leading to bounded orbits in phase space become more restricted with respect to initial separation. When the amplitudes are decreased, we found that the initial pulse separation could be larger and still lead to bounded, oscillatorlike orbits. These findings have been confirmed by the numerical simulations.

The phase difference $\Delta\sigma = 0$ is investigated next. Recall that the variational analysis of this case predicts a phenomenon not found by the perturbative analysis of the inverse scattering treatment. Specifically, the variational analysis predicts the existence of a transition from a repulsive to an attractive interaction, dependent upon the coupling coefficient between cores and the initial pulse amplitudes. We investigate this situation by generating the contour plots of the energy for a range of initial conditions. Figures 3 and 4 are contour plots for two different values of the coupling coefficient. In Fig. 3, when $\epsilon = 0.1$, and $\eta = 1.0$, any choice of initial condition for the pulse separation will result in a repulsive interaction; the phase-space origin is a saddle point. As the value of the coupling coefficient is increased to $\epsilon = 1$, however, bound states begin to emerge near the origin of the phase-space diagram. Initially the pulse separation corresponding to these bound states is confined to a narrow region near the origin; as the value of the coupling coefficient increases, so does the range of values for initial separation that will support an oscillatory state.

The results of the Hamiltonian analysis complement those predicted by the variational analysis. Both the attractive and repulsive interactions have been identified through this analysis. Moreover, the existence of a coupling coefficient dependent transition from a repulsive to attractive interaction is confirmed by this analysis. The Hamiltonian analysis further indicates that in the case of the so-called "attractive interaction," when either the initial separation or the initial velocity is sufficiently large, the bound-state interaction is not observed. The dependence of this transition on the initial pulse separation indicates that pulse overlap plays a key role in the interaction.

In order to more accurately consider what would truly

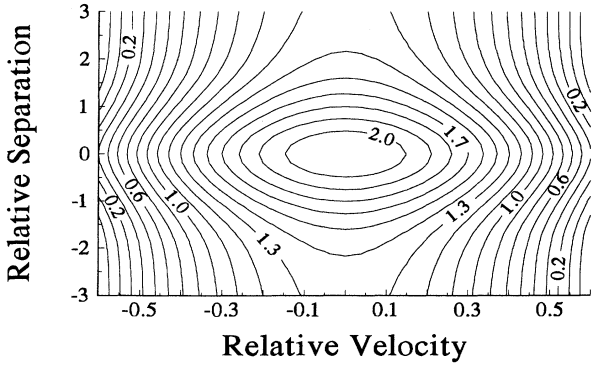

FIG. 1. Constant energy contours for the case $\Delta\sigma = \pi$, $\epsilon = 0.1$, and $\eta = 1.0$.

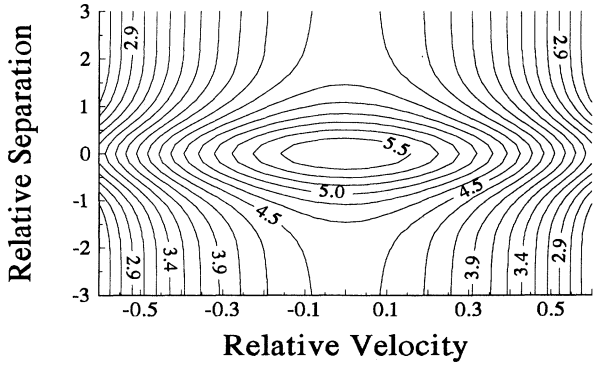

FIG. 2. Constant energy contours for the case $\Delta\sigma = \pi$, $\epsilon = 0.1$, and $\eta = 1.5$.

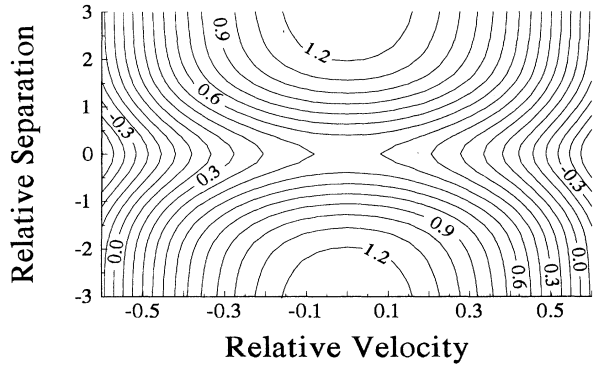

FIG. 3. Constant energy contours for the case $\Delta\sigma = 0$, $\epsilon = 0.1$, and $\eta = 1.0$.

occur in an experiment, as well as to ascertain the relative merits of analytical methods employed above, we compare these analytical results with those obtained by numerically evaluating the original CNLSEs [Eqs. (1) and (2)]. For clarity we first describe the method by which we solve the CNLSEs. We then will proceed to describe the results obtained from these simulations.

II. NUMERICAL METHODS

To numerically solve the CNLSEs, we use the split-step beam propagation method. The equations can be written in vector form as

$$\frac{\partial \mathbf{V}}{\partial z} = \mathbf{D}\mathbf{V} + \mathbf{N}\mathbf{V}, \tag{27}$$

where $\mathbf{D}$ is a linear operator whose form is given by

$$\mathbf{D} = \frac{i}{2}\frac{\partial^2 \sigma_0}{\partial t^2} - i\epsilon\sigma_1.$$

We define σ_0 and σ_1 as 2×2 matrix arrays given by

$$\sigma_0 = \begin{pmatrix} 1 & 0 \\ 0 & 1 \end{pmatrix}, \quad \sigma_1 = \begin{pmatrix} 0 & 1 \\ 1 & 0 \end{pmatrix}.$$

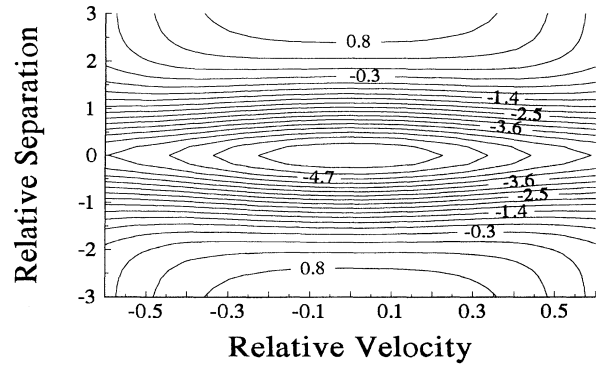

FIG. 4. Constant energy contours for the case $\Delta\sigma = 0$, $\epsilon = 1.0$, and $\eta = 1.0$.

We can then define the nonlinear operator $\mathbf{N}$ as

$$\mathbf{N} = i\begin{pmatrix} |\psi_1|^2 & 0 \\ 0 & |\psi_2|^2 \end{pmatrix}.$$

The formal solution of Eq. (27) is

$$\mathbf{V} = \mathbf{V}_0 \exp \int (\mathbf{D} + \mathbf{N}) dz. \tag{28}$$

The operators are separated by splitting the exponential into an approximate form given in the book by Agrawal [12]. The error is minimized by choosing Δz small enough; typically we choose values around 10^{-3}. The operators $\mathbf{D}$ are diagonalized by applying the fast Fourier transform algorithm. We use 2048 points in our program with a time window of 40. The advantage of this form of solution is that it is exact for the linear equation. Moreover, the nonlinear contribution is oscillatory and bounded; therefore it does not develop a runaway numerical instability.

To improve further on the accuracy of the evaluation of the nonlinear contribution to the integral, we employ an iterative procedure as described by Agrawal [12]. We found that two iterations of the algorithm provided sufficient convergence of the solution.

III. SIMULATION RESULTS FOR THE COUPLED NONLINEAR SCHRÖDINGER EQUATION

Following the algorithm outlined above, we proceed to test the analytical results. First, the existence of the attractive and repulsive interactions is verified and the results of AAD confirmed. Through the investigation, we found that the pulse shapes retained their hyperbolic secant form during the interaction. This was a verification of our trial functions with one caveat. The amplitudes η did change by approximately $10 - 20\,\%$ as the waves propagated through the fibers.

We proceed to investigate the discrepancies between the predictions reported by AAD and those obtained in the variational analysis. We note that the first difference arises in the derived period of oscillation for the attractive interaction as a function of coupling coefficient and initial amplitude (see Table II). To resolve this discrepancy we ran a series of models where we chose an initial phase difference of $\Delta\sigma = \pi$ (i.e., the phase condition whose solution always leads to the attractive interaction), a separation of $\Delta y = 2y = 1.2$ (normalized time units), and a coupling coefficient $\epsilon = 0.1$. Simulations for a range of pulse amplitudes (0.5–2.0) were run. In Fig. 5, we compare the oscillation periods obtained from these simulations with those obtained from AAD's analysis and those from the variational analysis. We note the predictions for the period of oscillation made by both analytical techniques as the initial amplitude increases. As the value for the initial amplitude decreases, differences between the two analytical techniques become evident. We note that the variational analysis provides a more

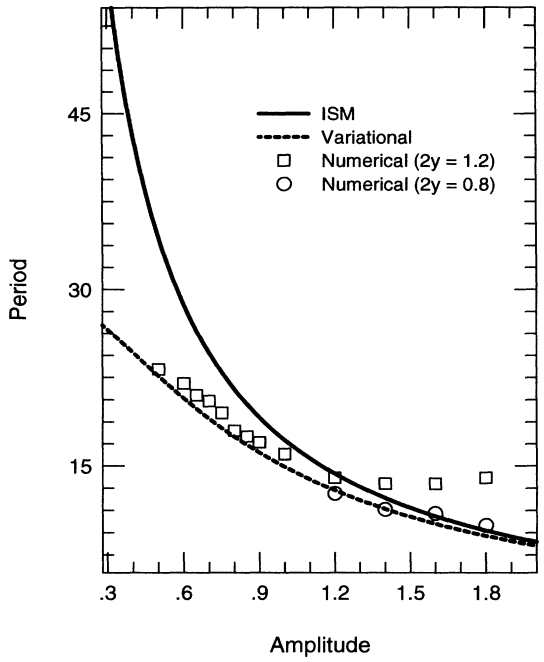

FIG. 5. Oscillation period as a function of initial amplitude and comparison of numerical results and analytical predictions.

accurate fit to the numerical results in the limit of small initial amplitude.

In the limit of large initial amplitude, however, the numerical results appear to differ significantly from the predictions of both the variational and perturbative techniques. This discrepancy can be understood physically in terms of pulse overlap. As the initial amplitudes become larger, the initial widths decrease. This corresponds to an effective increase in the pulse separation. Consequently, the evanescent field overlap decreases. In the numerical evaluation of the CNLSEs, this effect manifests itself in smaller values of the field on the second core being coupled to the fields on the first core. Furthermore, we recall from the Hamiltonian analysis that as pulse separations increase, the bound interactions diminish until the pulses eventually propagate independently of one another. To test whether our understanding is accurate, we ran the same models as above, decreasing the initial pulse separation distance to $\Delta y = 0.8$. By decreasing the pulse separation, we should satisfy the conditions of the linearized equations. With this approach, as seen via the Hamiltonian analysis, decreasing the initial pulse separation changes the orbit or phase-space trajectory and therefore the related periodicity of the interaction. We observe in Fig. 5 that by decreasing the initial separation of the pulses, the numerically computed periods begin to fit better the analytical predictions of the linearized equations of motion. In general, we find that in those cases where the perturbative technique differs from the variational predictions, the simulation results tend to be more consistent with the results obtained with the variational analysis. This indicates that the variational analysis is a more general analytical tool for these types of interactions.

The variational analysis further predicts that both the coupling coefficient ϵ and the initial phase difference $\Delta\sigma$ play a role in the types of interaction observed between two coupled solitons when the initial phase difference is given by $\Delta\sigma = 0, 2\pi, 4\pi, m\pi$, where m is an even integer. Specifically, for the case $0 < \epsilon < [3\eta^2/\pi^2]$, the pulses typically increase their separation exponentially as they propagate. However, when $\epsilon > [3\eta^2/\pi^2]$ and the same initial phase relationship is maintained, the pulses oscillate about a common center in what we have termed the attractive interaction. Furthermore, based on the information obtained from the variational analysis, if the coupling coefficient were chosen such that $\epsilon = [3\eta^2/\pi^2]$, it could be anticipated that the pulses would maintain their initial separation or at most separate as a linear function of the propagation distance. Recall that the perturbative analysis given by AAD assumed ϵ to be small and made no prediction about this crossover behavior.

To test the predictions we ran a series of simulations where the initial phase difference was given by $\Delta\sigma = 0$, the initial amplitude of the hyperbolic secant pulse shapes was $\eta = 1$, the initial separation between the pulses on adjacent cores of the dual-core fiber were given in normalized time units as $\Delta y = 1.2$, and we varied the value of the coupling coefficient from $\epsilon = 0.1$ to 1.0. The results of these simulations are shown in Figs. 6(b)–6(f), where we have plotted the pulse center on each core as a function of propagation distance ξ. To comple-

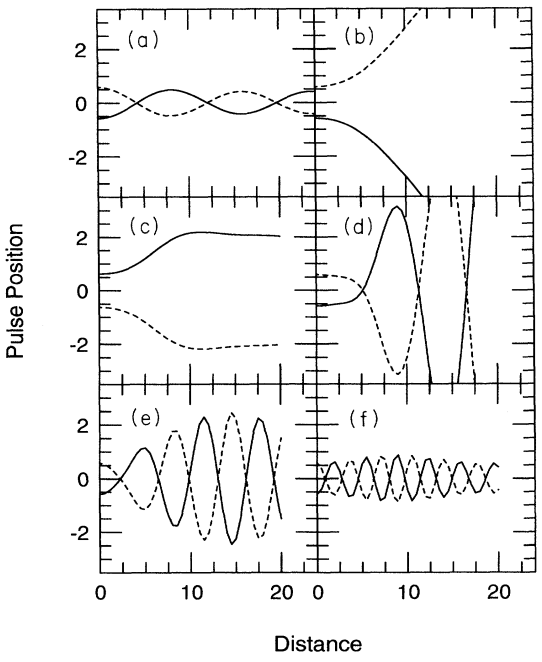

FIG. 6. Pulse position as a function of propagation distance. (a) $\Delta\sigma = \pi$, $\epsilon = 0.1$, and $\Delta y = 1.2$; (b) $\Delta\sigma = 0$, $\epsilon = 0.1$, and $\Delta y = 1.2$; (c) $\Delta\sigma = \pi$, $\epsilon = 0.165$, and $\Delta y = 1.2$; (d) $\Delta\sigma = \pi$, $\epsilon = 0.3$, and $\Delta y = 1.2$; (e) $\Delta\sigma = \pi$, $\epsilon = 0.5$, and $\Delta y = 1.2$; (f) $\Delta\sigma = \pi$, $\epsilon = 1.0$, and $\Delta y = 1.2$

ment these data, Fig. 6(a) shows a similar plot for the case $\eta = 1$, $\epsilon = 0.1$, and $\Delta\sigma = \pi$. The pulse center $\overline{T_i}$ is calculated for the pulse on each core i as

$$\overline{T_i} = \frac{\int T_i \left|\psi_i^2\right| dT}{\int \left|\psi_i^2\right| dT}. \tag{29}$$

For a symmetric pulse that maintains its shape, such as a solitonlike pulse, Eq. (29) should well approximate the position of the peak of that pulse.

When $\epsilon = 0.1$ [Fig. 6(b)] the pulses appear to increase their separation distance exponentially as a function of propagation distance in a manner consistent with prediction. When $\epsilon = 0.165$ [Fig. 6(c)], the pulses initially behave as in the preceding case; they separate as a function of propagation distance. However, at approximately $\xi = 10$, the pulse separation stabilizes and remains stabilized.

When the strength of the coupling coefficient is increased to $\epsilon = 0.3$ [Fig. 6(d)], we do not observe the expected constant separation of the pulses. Instead we observe an attractive, oscillatory interaction where the magnitude of the maximum pulse separation is much larger than the initial pulse separation and the maximum pulse separation over a single period of oscillation is not a constant throughout the propagation. This is contrasted with the nature of attractive interaction observed when the initial phase difference is $\Delta\sigma = \pi$; in that case, the pulse separations never exceed their initial value and generally maintain a constant value for the maximum pulse separation throughout the propagation. Additionally, it should be noted that the oscillations of the pulses about their common center is not periodic in the case of $\Delta\sigma = 0$ and $\epsilon = 0.3$. Instead, the pulses initially pull toward one another at a much slower rate, gradually decreasing the periodicity of the oscillation as the pulses propagate. This value for the coupling coefficient appears to correspond to a transition region between the repulsive and the attractive case.

When the coupling coefficient is increased further to $\epsilon = 0.5$, [Fig. 6(e)], we found that, though the rate of oscillation about a common center has increased, the oscillations continue to be aperiodic and the pulse separations during oscillation continue to exceed the initial pulse separation. As in the preceding case, the initial attractive interaction is much slower than would be predicted by an oscillator model. The variational analysis with linearized equations of motion predicts that this value of the coupling coefficient should correspond to an attractive interaction with a period of oscillation given by $3\pi/\sqrt{\epsilon(\pi^2\epsilon - 3\eta^2)}$. For our parameters, this corresponds to a value of 9.58. Toward the end of the propagation, $\xi > 15$, periodic oscillations appear. The period measured 7.0, significantly less than predicted. This discrepancy is due to the large pulse separations during oscillation. Finally, at $\epsilon = 1.0$ [Fig. 6(f)], the attractive interaction begins to resemble its counterpart for an initial phase difference of π. The oscillations appear to be smoothly periodic and approximately maintain their initial pulse separation during oscillation. Moreover, the periodicity of the oscillations, measured at 4.0, closely approximates the value predicted by the variational analysis, which is 3.59.

SUMMARY

In summary, we find both through analytical and numerical techniques that solitons launched on adjacent cores of dual-core fiber exhibit both an attractive and a repulsive interaction. Our results expand on an earlier paper of AAD. Specifically we find a coupling coefficient dependence to the nature of the soliton interactions that has possibilities for exploitation in switching devices. Our numerical results validate and more closely correlate with the findings of the variational formulation.

What remains is a discussion of a possible experimental test of our findings. Table I examines the range of coupling coefficients for a particular set of physical parameters of a dual-core fiber; the values of the core radius ρ_0 and the index difference Δn are typical values at the wavelength $\lambda = 1.55$ μm. When the core-to-core separation is around 40 μm and the pulse widths are 1 ps, the coupling coefficient is near unity. For the same parameter values and pulse widths of 250 fs, the coupling coefficient, according to Eqs. (3) and (4), will be 16 times smaller. This would enable an experiment to be designed to cover the repulsive and the attractive regimes. The length of fiber needed to observe the oscillations is around three dispersion lengths for $\epsilon = 1$ ($T_0 = 300$ fs). The dispersion length in the first instance is 50 m and the second is 3.125 m. In either case, about 150 m of fiber would be sufficient to observe a full oscillation period. The peak power required for the shortest pulses is about 18 W and for the longer pulses it is reduced to about 2 W.

ACKNOWLEDGMENTS

This research was supported in part by the Department of Education and in part by a U.S. Army Research Grant Contract No. DAAH04-93-G-0079. R.L.F. gratefully acknowledges support for this work from AFOSR under Grant No. F49620-92-J-0456. Initial discussions with James Theimer and Steven Doty are gratefully acknowledged.

[1] S. Jensen, IEEE J. Quantum Electron. **QE-18**, 1580 (1982).
[2] P. Chu, G. D. Peng, and B. Malomed, Opt. Lett. **18**, 328 (1993).
[3] T. Ueda and W. L. Kath, Phys. Rev. A **42**, 563 (1990).
[4] F. Kh. Abdullaev, R. M. Abrarov, and S. A. Darmanyan, Opt. Lett. **14**, 131 (1989).
[5] K. J. Blow and N. J. Doran, Electron. Lett. **19**, 429

(1983).
[6] J. P. Gordon, Opt. Lett. **8**, 596 (1983).
[7] D. Anderson, Phys. Rev. A **27**, 3135 (1983).
[8] D. Anderson and M. Lisak, Phys. Rev. A **32**, 2270 (1985).
[9] D. Anderson, M. Lisak, and T. Reichel, Phys Rev. A **38**, 1618 (1988).
[10] C. Pare and M. Florjanczyk, Phys. Rev. A **41**, 6287 (1990).
[11] A. W. Snyder and J. D. Love, *Optical Waveguide Theory* (Chapman and Hall, London, 1983), Chaps. 12–15.
[12] G. P. Agrawal, *Nonlinear Fiber Optics* (Academic, San Diego, 1989).
[13] G. P. Agrawal, *Fiber Optic Communication Systems* (Academic, New York, 1992).